

1 **SARS-CoV-2 B.1.1.7 escape from mRNA vaccine-elicited neutralizing antibodies**

2

3 Dami A. Collier^{1,2,3*}, Anna De Marco^{4*}, Isabella A.T.M. Ferreira^{*1,2} Bo Meng^{1,2*}, Rawlings
4 Datir ^{*1,2,3}, Alexandra C. Walls⁵, Steven A. Kemp S^{1,2,3}, Jessica Bassi⁴, Dora Pinto⁴, Chiara
5 Silacci Fregni⁴, Siro Bianchi⁴, M. Alejandra Tortorici⁵, John Bowen⁵, Katja Culap⁴, Stefano
6 Jaconi⁴, Elisabetta Cameroni⁴, Gyorgy Snell⁶, Matteo S. Pizzuto⁴, Alessandra Franzetti
7 Pellanda⁷, Christian Garzoni⁷, Agostino Riva⁸, The CITIID-NIHR BioResource COVID-19
8 Collaboration⁹, Anne Elmer¹⁰, Nathalie Kingston¹⁰, Barbara Graves¹⁰, Laura E McCoy³,
9 Kenneth GC Smith^{1,2}, John R. Bradley^{2,10}, Lourdes Ceron-Gutierrez L¹¹, Gabriela Barcenas-
10 Morales^{11,12}, The COVID-19 Genomics UK (COG-UK) consortium¹³, William Harvey¹⁴,
11 Herbert W. Virgin⁶, Antonio Lanzavecchia⁴, Luca Piccoli⁴, Rainer Doffinger¹¹, Mark Wills²,
12 David Veesler⁵, Davide Corti^{4*}, Ravindra K. Gupta^{1,2, 15*}

13

14 *Equal contribution

15

16 ¹Cambridge Institute of Therapeutic Immunology & Infectious Disease (CITIID), Cambridge, UK.

17 ²Department of Medicine, University of Cambridge, Cambridge, UK.

18 ³Division of Infection and Immunity, University College London, London, UK.

19 ⁴Humabs Biomed SA, a subsidiary of Vir Biotechnology, 6500 Bellinzona, Switzerland.

20 ⁵Department of Biochemistry, University of Washington, Seattle, WA 98195, USA

21 ⁶Vir Biotechnology, San Francisco, CA 94158, USA.

22 ⁷Clinic of Internal Medicine and Infectious Diseases, Clinica Luganese Moncucco, 6900 Lugano,
23 Switzerland

24 ⁸Division of Infectious Diseases, ASST Fatebenefratelli Sacco, Luigi Sacco Hospital, University of
25 Milan, 20157 Milan, Italy

26 ⁹The CITIID-NIHR BioResource COVID-19 Collaboration, see appendix 1 for author list

27 ¹⁰NIHR Cambridge Clinical Research Facility, Cambridge, UK.

28 ¹¹Department of Clinical Biochemistry and Immunology, Addenbrookes Hospital, UK

29 ¹²Laboratorio de Inmunología, S-Cuautitlán, UNAM, Mexico

30 ¹³<https://www.cogconsortium.uk>. Full list of consortium names and affiliations are in Appendix 2.

31 ¹⁴ Institute of Biodiversity, Animal Health and Comparative Medicine, University of Glasgow,
32 Glasgow, UK

33 ¹⁵ Africa Health Research Institute, Durban, South Africa

34

35

36 **Correspondence:** dcorti@vir.bio, rkg20@cam.ac.uk

37

38 **Key words:** SARS-CoV-2; COVID-19; antibody, vaccine, neutralising antibodies;
39 **mutation;**

40

41 Abstract

42 SARS-CoV-2 transmission is uncontrolled in many parts of the world, compounded in
43 some areas by higher transmission potential of the B.1.1.7 variant now seen in 50
44 countries. It is unclear whether responses to SARS-CoV-2 vaccines based on the
45 prototypic strain will be impacted by mutations found in B.1.1.7. Here we assessed
46 immune responses following vaccination with mRNA-based vaccine BNT162b2. We
47 measured neutralising antibody responses following a single immunization using
48 pseudoviruses expressing the wild-type Spike protein or the 8 mutations found in the
49 B.1.1.7 Spike protein. The vaccine sera exhibited a broad range of neutralizing titres
50 against the wild-type pseudoviruses that were modestly reduced against B.1.1.7 variant.
51 This reduction was also evident in sera from some convalescent patients. Decreased
52 B.1.1.7 neutralization was also observed with monoclonal antibodies targeting the N-
53 terminal domain (9 out of 10), the Receptor Binding Motif (RBM) (5 out of 29), but not
54 in neutralizing mAbs binding outside the RBM. Introduction of the E484K mutation in
55 a B.1.1.7 background to reflect newly emerging viruses in the UK led to a more
56 substantial loss of neutralizing activity by vaccine-elicited antibodies over that conferred
57 by the B.1.1.7 mutations alone. Further work is needed to establish the impact of these
58 observations on protective vaccine efficacy in the context of the evolving B.1.1.7 lineage.

60 Introduction

61 The outbreak of a pneumonia of unknown cause in Wuhan, China in December 2019,
62 culminated in a global pandemic due to a novel viral pathogen, now known to be SARS-
63 COV-2¹. The unprecedented scientific response to this global challenge has led to the rapid
64 development of vaccines aimed at preventing SARS-COV-2 infection and transmission.
65 Continued viral evolution led to the emergence and selection of SARS-CoV-2 variants with
66 enhanced infectivity/transmissibility^{2,3 4,5} and ability to circumvent drug⁶ and immune
67 control^{7,8}.

68 SARS-CoV-2 vaccines have recently been licensed that target the Spike (S) protein,
69 either using mRNA or adenovirus vector technology with protection rates over a few months
70 ranging from 62 to 95%⁹⁻¹¹. The BNT162b2 vaccine encodes the full-length trimerised S
71 protein of SARS CoV-2 and is formulated in lipid nanoparticles to optimise delivery to
72 cells¹². Other vaccines include the Moderna mRNA-1273 vaccine, which is also a lipid
73 nanoparticle formulated S glycoprotein¹³ and the Oxford-AstraZeneca ChAdOx1 nCoV-19
74 vaccine (AZD1222) which is a replication-deficient chimpanzee adenoviral vector ChAdOx1,
75 containing the S glycoprotein¹⁴. The duration of immunity conferred by these vaccines is as
76 yet unknown. These vaccines were designed against the Wuhan-1 isolate discovered in 2019.
77 Concerns have been raised as to whether these vaccines will be effective against new SARS-
78 CoV-2 variants, such as B.1.1.7 (N501Y.V1), B.1.351 (N501Y.V2) and P1 (N501Y.V2) that

79 originated in the UK, South Africa, and Brazil and are now being detected all over the
80 world¹⁵⁻¹⁷.

81 The phase I/II studies of the Pfizer-BioNTech BNT162b2 vaccine determined the
82 immunogenicity of different dosing regimens. The geometric mean concentration (GMC) of
83 RBD-binding IgG 21 days after the first dose of 30 µg of the BNT162b2 vaccine, which is the
84 dose approved in the UK, was higher than the GMC of a panel of convalescent plasma (1,536
85 vs 602 U/ml). Nevertheless, the corresponding neutralisation geometric mean titre (GMT) was
86 3-fold lower than a panel of convalescent plasma (29 vs 94)¹², but substantially increased after
87 boost immunization¹⁸. In older adults mean GMT was only 12 in a preliminary analysis of 12
88 participants¹⁹ and increased to 109 after the second dose.

89 In this study, we assess antibody responses induced three weeks after vaccination with
90 the first dose of BNT162b2 following the rollout in the UK. In addition, by using a panel of
91 human neutralizing monoclonal antibodies (mAbs) we show that the B.1.1.7 variant can
92 escape neutralization mediated by most NTD-specific antibodies tested and by a fraction of
93 RBM-specific antibodies. We also show that the recent appearance of the E484K mutation in
94 B.1.1.7 isolates from the UK, similarly to the B.1.351 and P1 isolates, results in incremental
95 loss of neutralization by BNT162b2 mRNA-elicited antibodies.

96

97 **Results**

98 Twenty-four participants had received the BNT162b2 mRNA vaccine three weeks prior to
99 blood draw for serum and peripheral blood mononuclear cells (PBMC) collection. Median age
100 was 82 years (IQR 64-85) and 30% were female (**Supplementary Table 1**). Serum IgG titres
101 to N protein, S and the S RBD were assayed by particle based flow cytometry on a Luminex
102 analyser (**Fig. 1a**). These data showed Spike and RBD antibody titres much higher than in
103 healthy controls, similar to both convalescent plasma units used for therapeutic purposes as
104 well as to serum from recovered individuals. The raised N titres relative to control could be
105 the result of non specific cross reactivity that is increased following vaccination. However, the
106 antibody response was heterogeneous with almost 100-fold variation in IgG titres to S and
107 Spike RBD across the vaccinated participants.

108 Using lentiviral pseudotyping we generated wild type S proteins on the surface of enveloped
109 virions in order to measure neutralisation activity of vaccine-elicited sera. This system has
110 been shown to give results correlating with replication competent authentic virus^{20,21}. The

111 vaccine sera exhibited a range of inhibitory dilutions giving 50% neutralisation (ID₅₀) (**Fig.**
112 **1c-d**). The GMT against wild type (WT) pseudovirus was 24. Seven out of 23 participants
113 exhibited no appreciable neutralisation against the WT pseudotyped virus. There was
114 reasonable correlation between full length S IgG titres and serum neutralisation titres
115 (**Extended Data Fig. 1a**). A broad range of T cell responses was measured by IFN gamma
116 FLUOROSPOT against SARS-CoV-2 peptides in vaccinees. These cell responses did not
117 correlate with IgG S antibody titres, but there was some correlation with serum neutralisation
118 against WT virus (**Extended Data Fig. 1b-c**).

119 We next generated mutated pseudoviruses carrying S protein with mutations N501Y,
120 A570D and the H69/V70 deletion. We observed no reduction in the ability of sera from
121 vaccinees to inhibit either WT or mutant virus (**Extended Data Fig. 2**). In fact, we observed
122 that vaccine sera displayed higher neutralizing activity against the N501Y, A570D and
123 H69/V70 deletion mutant relative to WT virus. Next, we then tested a panel of sera from 11
124 recovered individuals and found that these sera also neutralised both wild type and the
125 mutated viruses similarly (**Extended Data Fig. 3**). The findings for vaccine sera may be
126 related to a potential allosteric effect of Δ H69/V70 that might enhance neutralization by
127 antibodies targeting cryptic sites on the S, such as the RBD site II (also named as class 4 site).

128 We then generated the full set of eight mutations in the S protein present in B.1.1.7
129 variant (**Fig. 1b** and **Table 1**), Δ H69/V70, Δ 144, N501Y and A570D in the S₁ subunit and
130 P681H, T716I, S982A and D1118H in the S₂ subunit. All constructs also contained D614G.
131 We found that among 15 individuals with neutralisation activity three weeks after receiving a
132 single dose of the the BNT162b2 mRNA vaccine, 10 showed evidence of reduction in
133 efficacy of antibodies against the B.1.1.7 mutant (**Fig. 1c-d**). The highest fold change was
134 approximately 6. Amongst sera from 7 recovered individuals, only 2 demonstrated reduced
135 potency against B.1.1.7 (**Fig. 1e-h** and **Extended Data Fig. 4**).

136 **B.1.1.7 variant escapes from NTD- and RBM-specific mAb-mediated neutralization.**

137 To investigate the role of the full set of mutations in NTD, RBD and S₂ present in the B.1.1.7
138 variant, we tested 61 mAbs isolated from 15 individuals that recovered from WT SARS-
139 CoV-2 infection with an *in-vitro* pseudotyped neutralization assay using VeroE6 target cells
140 expressing TMPRSS2 (**Extended Data Table 1**). We found that 20 out of 61 (32.8%) mAbs
141 showed a greater than 2-fold loss of neutralizing activity of B.1.1.7 variant compared to WT

142 SARS-CoV-2 (**Fig. 2a,b** and **Extended Data Fig. 5**). Remarkably, the B.1.1.7 mutant virus
143 was found to fully escape neutralization by 7 out of 10 NTD-targeting mAbs (70%), and
144 partial escape from additional 2 mAbs (20%) (**Fig. 2c**). We previously showed that the
145 deletion of residue 144 abrogates binding by 4 out of 6 NTD-specific mAbs tested, possibly
146 accounting for viral neutralization escape by most NTD-specific antibodies²². Of the 29
147 RBM-targeting mAbs, 5 (17.2%) showed more than 100-fold decrease in B.1.1.7
148 neutralization, and additional 6 mAbs (20.7%) had a partial 2-to-10-fold reduction (**Fig. 2d**).
149 Finally, all RBD-specific non-RBM-targeting mAbs tested fully retained B.1.1.7 neutralizing
150 activity (**Fig. 2e**).

151 To address the role of B.1.1.7 N501Y mutation in the neutralization escape from
152 RBM-specific antibodies, we tested the binding of 51 RBD-specific mAbs to WT and N501Y
153 mutant RBD by biolayer interferometry (**Fig. 2f** and **Extended Data Fig. 6**). The 5 RBM-
154 specific mAbs that failed to neutralize B.1.1.7 variant (**Fig. 2d**) showed a complete loss of
155 binding to N501Y RBD mutant (**Fig. 2g, h**), demonstrating a critical role for this mutation as
156 an escape mechanism for RBM-targeting mAbs.

157 The decreased neutralizing activity of the immune sera from vaccinees and
158 convalescent patients against B.1.1.7, but not against Δ 69/70-501Y-570D mutant (**Fig. 1** and
159 **Extended Data Fig. 2**), could be the result of a loss of neutralizing activity of both RBD- and
160 NTD-targeting antibodies, and suggests that the key mutations driving polyclonal escape are
161 Δ 144 and N501Y.

162

163 SARS-CoV-2 B.1.1.7 binds human ACE2 with higher affinity than WT

164 SARS-CoV-2 and SARS-CoV enter host cells through binding of the S glycoprotein to
165 ACE2^{1,23}. Previous studies showed that the binding affinity of SARS-CoV for human ACE2
166 correlated with the rate of viral replication in distinct species, transmissibility and disease
167 severity²⁴⁻²⁶. To understand the potential contribution of receptor interaction to infectivity,
168 we set out to evaluate the influence of the B.1.1.7 RBD substitution N501Y on receptor
169 engagement. We used biolayer interferometry to study binding kinetics and affinity of the
170 purified human ACE2 ectodomain (residues 1-615) to immobilized biotinylated SARS-CoV-
171 2 B.1.1.7 or WT RBDs. We found that ACE2 bound to the B.1.1.7 RBD with an affinity of
172 22 nM compared to 133 nM for the WT RBD (**Extended Data Fig. 7**), in agreement with our
173 previous deep-mutational scanning measurements using dimeric ACE2²⁷. Although ACE2
174 bound with comparable on-rates to both RBDs, the observed dissociation rate constant was
175 slower for B.1.1.7 than for the WT RBD (**Table 2**). Enhanced binding of the B.1.1.7 RBD to

176 human ACE2 resulting from the N501Y mutation might participate to the efficient ongoing
177 transmission of this newly emerged SARS-CoV-2 lineage, and possibly reduced opportunity
178 for antibody binding.

179

180 **Further loss of neutralization of vaccine-elicited antibodies against a B.1.1.7 Spike**
181 **carrying E484K mutation**

182 The E484K substitution (**Fig 3a**) has been identified as antigenically important, being
183 reported as an escape mutation for several monoclonal antibodies including C121, C144,
184 REGN10933 and REGN10934. E484K is also known to be present in the B.1.351 (501Y.V2)
185 and the P.1 (501Y.V3) lineages in combination with amino acid replacements at N501 and
186 K417. As of 1st Feb 2021, fourteen English and two Welsh B.1.1.7 sequences from viral
187 isolates contained the E484K substitution (**Fig. 3b**), The number of B.1.1.7 sequences has
188 been increasing since the start of December 2020 (**Fig. 3c**). Phylogenetic analysis suggests
189 that there were two independent acquisitions in English and Welsh sequences (**Fig. 3b**).

190 We generated pseudoviruses bearing B.1.1.7 Spike mutations with or without additional
191 E484K and tested these against vaccine sera. We observed a significant loss of neutralising
192 activity compared with WT and with B.1.1.7; mean fold change for the E484K B.1.1.7 Spike
193 was 9.6 compared to 2.4 for B.1.1.7 alone ($p < 0.05$) (**Fig. 4**).

194 Discussion

195 Serum neutralizing activity is a correlate of protection for other respiratory viruses, including
196 influenza²⁸ and respiratory syncytial virus where prophylaxis with monoclonal antibodies has
197 been used in at-risk groups^{29,30}. Neutralising antibody titres appeared to be highly correlated
198 with vaccine protection against SARS-CoV-2 rechallenge in non-human primates, and
199 importantly, there was no correlation between T cell responses (as measured by ELISPOT)
200 and protection³¹. Moreover, passive transfer of purified polyclonal IgGs from convalescent
201 macaques protected naïve macaques against subsequent SARS-CoV-2 challenge³². Coupled
202 with multiple reports of re-infection, there has therefore been significant attention placed on
203 virus neutralisation.

204 This study reports on the neutralisation escape from sera collected after one dose of
205 the BNT162b2 vaccine. The participants of this study had a median age of over 80, in line
206 with the targeting of this age group in the initial rollout of the vaccination campaign in the
207 UK. Participants showed similar neutralising activity against wild type pseudovirus as in the
208 phase I/II study, with geometric mean titres of 24 and 29, respectively¹². The three mutations
209 in S (N501Y, A570D, Δ H69/V70) did not appear to impact neutralisation in a pseudovirus
210 assay. However, we demonstrated that a pseudovirus bearing S protein with the full set of
211 mutations present in the B.1.1.7 variant (i.e., Δ H69/V70, Δ I144, N501Y, A570D, P681H,
212 T716I, S982A, D1118H) did result in small reduction in neutralisation by sera from
213 vaccinees. A reduction in neutralization titres from mRNA-elicited antibodies in volunteers
214 who received two doses (using both mRNA-1273 and BNT162b2 vaccines) was also
215 observed by Wang et al.³³ using pseudoviruses carrying the N501Y mutation. Another study
216 reported on a modest and not significant (average 1.2 fold) reduction of neutralization against
217 the B.1.1.7 variant in sera from individuals vaccinated with two doses of mRNA-1273³⁴. The
218 level of neutralizing antibodies observed in both of these studies was approximately one log
219 higher than the one observed in the cohort of vaccinees described in this study. This may be
220 related to the older age of the individuals from this study as well as to the fact that these were
221 exposed to only one dose of the BNT162b2 vaccine. In general, it is expected that the effect
222 of mutations on the neutralization by polyclonal serum antibodies might be more prominent
223 on low-titre in contrast to high-titre sera. It is important to study virus neutralisation at lower
224 serum neutralisation titres because decline in neutralisation titres over time is expected to
225 occur following vaccination.

226 The reduced neutralizing activity observed with polyclonal antibodies elicited by
227 mRNA vaccines observed in this study and in Wang et al.³³ is further supported by the loss of
228 neutralizing activity observed with human mAbs directed to both RBD and, to a major extent,
229 to NTD. In the study by Wang et al., 6 out of 17 RBD-specific mAbs isolated from mRNA-1273
230 vaccinated individuals showed more than 100-fold neutralization loss against N501Y mutant,
231 a finding that is consistent with the loss of neutralization by 5 out of 29 RBM-specific mAbs
232 described in this study.

233 Multiple variants, including the 501Y.V2 and B.1.1.7 lineages, harbor multiple
234 mutations as well as deletions in NTD, most of which are located in a site of vulnerability that
235 is targeted by all known NTD-specific neutralizing antibodies²². The role of NTD-specific
236 neutralizing antibodies might be under-estimated, in part by the use of neutralization assays
237 based on target cells over-expressing ACE2 receptor. NTD-specific mAbs were suggested to
238 interfere with viral entry based on other accessory receptors, such as DC-SIGN and L-SIGN³⁵,
239 and their neutralization potency was found to be dependent on different in vitro culture
240 conditions²². The observation that 9 out of 10 NTD-specific neutralizing antibodies failed to
241 show a complete or near-complete loss of neutralizing activity against B.1.1.7 indicates that
242 this new variant may have evolved also to escape from this class of antibodies, that may have
243 a yet unrecognized role in protective immunity. Wibmer et al.³⁶ have also recently reported
244 the loss of neutralization of 501Y.V2 by the NTD-specific mAb 4A8, likely driven by the
245 R246I mutation. This result is in line with the lack of neutralization of B.1.1.7 by 4A8 mAb
246 observed in this study, likely caused by Δ 144 due to loss of binding²². Finally, the role of
247 NTD mutations (in particular, L18F, Δ 242-244 and R246I) was further supported by the
248 marked loss of neutralization observed by Wibmer et al.³⁶ against 501Y.V2 compared to the
249 chimeric virus carrying only the RBD mutations K417N, E484K and N501Y. Taken together,
250 the presence of multiple escape mutations in NTD is supportive of the hypothesis that this
251 region of the Spike, in addition to RBM, is also under immune pressure.

252 E484K has been shown to impact neutralisation by monoclonal antibodies or
253 convalescent sera, especially in combination with N501Y and K417N^{16,37-39}. Worryingly, we
254 have shown that there are multiple B.1.1.7 sequences in the UK bearing E484K with early
255 evidence of transmission as well as independent acquisitions. We measured further reduction
256 neutralisation titers by vaccine sera when E484K was present alongside the B.1.1.7 S
257 mutations. Consistent with our findings, Wu and co-authors³⁴ have shown that variants

258 carrying the E484K mutation resulted in 3-to-6 fold reduction in neutralization by sera from
259 mRNA-1273 vaccinated individuals.

260 Evidence for the importance role of NTD deletions in combination with E484K in immune
261 escape is provided by Andreano *et al.* who describe the emergence of $\Delta 140$ in virus co-
262 incubated with potently neutralizing convalescent plasma, causing a 4-fold reduction in
263 neutralization titre. This $\Delta 140$ mutant subsequently acquired E484K which resulted in a
264 further 4-fold drop in neutralization titre indicating a two residue change across NTD and
265 RBD represents an effective pathway of escape that can dramatically inhibit the polyclonal
266 response.

267 Our study was limited by relatively small sample size. Although the Spike pseudotyping
268 system has been shown to faithfully represent full length infectious virus, there may be
269 determinants outside the S that influence escape from antibody neutralization either directly
270 or indirectly in a live replication competent system. On the other hand live virus systems
271 allow replication and therefore mutation to occur, and rigorous sequencing at multiple steps is
272 needed.

273 Amidst high transmission in many parts of the world, vaccines are a key part of a long term
274 strategy to bring SARS-CoV-2 under control. Our data suggest that vaccine escape will be
275 inevitable in the future, and should be mitigated by designing next generation vaccines with
276 mutated S sequences and using alternative viral antigens. Currently however, vaccines are
277 likely to contribute controlling SARS-CoV-2 infections in the short term.

278

279 **Acknowledgements**

280 We would like to thank Cambridge University Hospitals NHS Trust Occupational Health
281 Department. We would also like to thank the NIHR Cambridge Clinical Research Facility
282 and staff at CUH and. We would like to thank Eleanor Lim and Georgina Okecha. We thank
283 Dr James Voss for the kind gift of HeLa cells stably expressing ACE2. RKG is supported by a
284 Wellcome Trust Senior Fellowship in Clinical Science (WT108082AIA). LEM is supported
285 by a Medical Research Council Career Development Award (MR/R008698/1). SAK is
286 supported by the Bill and Melinda Gates Foundation via PANGEA grant: OPP1175094. DAC
287 is supported by a Wellcome Trust Clinical PhD Research Fellowship. KGCS is the recipient

288 of a Wellcome Investigator Award (200871/Z/16/Z). This research was supported by the
289 National Institute for Health Research (NIHR) Cambridge Biomedical Research Centre, the
290 Cambridge Clinical Trials Unit (CCTU), and the NIHR BioResource. The views expressed
291 are those of the authors and not necessarily those of the NIHR or the Department of Health
292 and Social Care. JAGB is supported by the Medical Research Council (MC_UP_1201/16).
293 IATM is funded by a SANTHE award.

294

295 **Author contributions**

296 Conceived study: D.C., RKG, DAC. Designed study and experiments: RKG, DAC, LEM, JB,
297 MW, JT, LCG, GBM, RD, BG, NK, AE, M.P., D.V., L.P., A.D.M, J.B., D.C. Performed
298 experiments: BM, DAC, RD, IATMF, LCG, GBM. Interpreted data: RKG, DAC, BM, RD,
299 IATMF, LEM, JB, KGCS. A.D.M., J.B. and C.S.F. carried out pseudovirus neutralization
300 assays. D.P. produced pseudoviruses. M.S.P., L.P., D.V. and D.C. designed the experiments.
301 A.C.W., N.S. and S.J. expressed and purified the proteins. K.C., S.J. and E.C. sequenced and
302 expressed antibodies. E.C. and K.C. performed mutagenesis for mutant expression plasmids.
303 A.C.W. M.A.T., J.E.B., and S.B. performed binding assays. A.R., A.F.P and C.G contributed
304 to donor's recruitment and sample collection related to mAbs isolation. H.W.V., G.S., A.L.,
305 D.V., L.P. and D.C. analyzed the data and prepared the manuscript with input from all
306 authors.

307 **Competing interests**

308 A.D.M., J.B., D.P., C.S.F., S.B., K.C., N.S., E.C., G.S., S.J., A.L., H.W.V., M.S.P., L.P. and
309 D.C. are employees of Vir Biotechnology and may hold shares in Vir Biotechnology. H.W.V.
310 is a founder of PierianDx and Casma Therapeutics. Neither company provided funding for
311 this work or is performing related work. D.V. is a consultant for Vir Biotechnology Inc. The
312 Veesler laboratory has received a sponsored research agreement from Vir Biotechnology Inc.
313 The remaining authors declare that the research was conducted in the absence of any
314 commercial or financial relationships that could be construed as a potential conflict of
315 interest. RKG has received consulting fees from UMOVIS Lab, Gilead and ViiV.

316

317 **MATERIALS AND METHODS**

318 *Participant recruitment and ethics*

319 Participants who had received the first dose of vaccine and individuals with COVID-19 were
320 consented into the Covid-19 cohort of the NIHR Bioresource. The study was approved by the
321 East of England – Cambridge Central Research Ethics Committee (17/EE/0025).

322

323 *SARS-CoV-2 serology by multiplex particle-based flow cytometry (Luminex):*

324 Recombinant SARS-CoV-2 N, S and RBD were covalently coupled to distinct carboxylated
325 bead sets (Luminex; Netherlands) to form a 3-plex and analyzed as previously described
326 (Xiong et al. 2020). Specific binding was reported as mean fluorescence intensities (MFI).

327

328 *Recombinant expression of SARS-CoV-2-specific mAbs.*

329 Human mAbs were isolated from plasma cells or memory B cells of SARS-CoV-2 immune
330 donors, as previously described⁴⁰⁻⁴². Recombinant antibodies were expressed in ExpiCHO
331 cells at 37°C and 8% CO₂. Cells were transfected using ExpiFectamine. Transfected cells
332 were supplemented 1 day after transfection with ExpiCHO Feed and ExpiFectamine CHO
333 Enhancer. Cell culture supernatant was collected eight days after transfection and filtered
334 through a 0.2 µm filter. Recombinant antibodies were affinity purified on an ÄKTA xpress
335 FPLC device using 5 mL HiTrap™ MabSelect™ Prisma columns followed by buffer
336 exchange to Histidine buffer (20 mM Histidine, 8% sucrose, pH 6) using HiPrep 26/10
337 desalting columns

338

339 *Generation of S mutants*

340 Amino acid substitutions were introduced into the D614G pCDNA_SARS-CoV-2_S plasmid
341 as previously described⁴³ using the QuikChange Lightning Site-Directed Mutagenesis kit,
342 following the manufacturer's instructions (Agilent Technologies, Inc., Santa Clara, CA).
343 Sequences were checked by Sanger sequencing.

344 Preparation of B.1.1.7 SARS-CoV-2 S glycoprotein-encoding-plasmid used to produce
345 SARS-CoV-2-MLV based on overlap extension PCR. Briefly, a modification of the overlap
346 extension PCR protocol⁴⁴ was used to introduce the nine mutations of the B.1.1.7 lineage in
347 the SARS-CoV-2 S gene. In a first step, 9 DNA fragments with overlap sequences were
348 amplified by PCR from a plasmid (phCMV1, Genlantis) encoding the full-length SARS-
349 CoV-2 S gene (BetaCoV/Wuhan-Hu-1/2019, accession number mn908947). The
350 mutations (del-69/70, del-144, N501Y, A570D, D614G, P681H, S982A, T716I and
351 D1118H) were introduced by amplification with primers with similar Tm. Deletion of the C-
352 terminal 21 amino acids was introduced to increase surface expression of the recombinant

353 S⁴⁵. Next, 3 contiguous overlapping fragments were fused by a first overlap PCR (step
354 2) using the utmost external primers of each set, resulting in 3 larger fragments with
355 overlapping sequences. A final overlap PCR (step 3) was performed on the 3 large
356 fragments using the utmost external primers to amplify the full-length S gene and the
357 flanking sequences including the restriction sites KpnI and NotI. This fragment was digested
358 and cloned into the expression plasmid pHCMV1. For all PCR reactions the Q5 Hot Start
359 High fidelity DNA polymerase was used (New England Biolabs Inc.), according to the
360 manufacturer's instructions and adapting the elongation time to the size of the amplicon.
361 After each PCR step the amplified regions were separated on agarose gel and purified
362 using Illustra GFX™ PCR DNA and Gel Band Purification Kit (Merck KGaA).

363

364 *Pseudotype virus preparation*

365 Viral vectors were prepared by transfection of 293T cells by using Fugene HD transfection
366 reagent (Promega). 293T cells were transfected with a mixture of 11ul of Fugene HD, 1μg of
367 pCDNAΔ19Spike-HA, 1ug of p8.91 HIV-1 gag-pol expression vector^{46,47}, and 1.5μg of
368 pCSFLW (expressing the firefly luciferase reporter gene with the HIV-1 packaging signal).
369 Viral supernatant was collected at 48 and 72h after transfection, filtered through 0.45um filter
370 and stored at -80°C. The 50% tissue culture infectious dose (TCID₅₀) of SARS-CoV-2
371 pseudovirus was determined using Steady-Glo Luciferase assay system (Promega).

372

373 *Serum/plasma pseudotype neutralization assay*

374 Spike pseudotype assays have been shown to have similar characteristics as neutralisation
375 testing using fully infectious wild type SARS-CoV-2²⁰. Virus neutralisation assays were
376 performed on 293T cell transiently transfected with ACE2 and TMPRSS2 using SARS-CoV-
377 2 Spike pseudotyped virus expressing luciferase⁴⁸. Pseudotyped virus was incubated with
378 serial dilution of heat inactivated human serum samples or sera from vaccinees in duplicate
379 for 1h at 37°C. Virus and cell only controls were also included. Then, freshly trypsinized
380 293T ACE2/TMPRSS2 expressing cells were added to each well. Following 48h incubation
381 in a 5% CO₂ environment at 37°C, luminescence was measured using the Steady-Glo
382 Luciferase assay system (Promega).

383 *IFN γ FLUOROSPOT assays*

384 Frozen PBMCs were rapidly thawed, and the freezing medium was diluted into 10ml of
385 TexMACS media (Miltenyi Biotech), centrifuged and resuspended in 10ml of fresh media
386 with 10U/ml DNase (Benzonase, Merck-Millipore via Sigma-Aldrich), PBMCs were
387 incubated at 37°C for 1h, followed by centrifugation and resuspension in fresh media
388 supplemented with 5% Human AB serum (Sigma Aldrich) before being counted. PBMCs
389 were stained with 2ul of each antibody: anti-CD3-fluorescein isothiocyanate (FITC), clone
390 UCHT1; anti-CD4-phycoerythrin (PE), clone RPA-T4; anti-CD8a-peridinin-chlorophyll
391 protein - cyanine 5.5 (PerCP Cy5.5), clone RPA-8a (all BioLegend, London, UK),
392 LIVE/DEAD Fixable Far Red Dead Cell Stain Kit (Thermo Fisher Scientific). PBMC
393 phenotyping was performed on the BD Accuri C6 flow cytometer. Data were analysed with
394 FlowJo v10 (Becton Dickinson, Wokingham, UK). 1.5 to 2.5 x 10⁵ PBMCs were incubated
395 in pre-coated Fluorospot plates (Human IFN γ FLUOROSPOT (Mabtech AB, Nacka Strand,
396 Sweden)) in triplicate with peptide mixes specific for Spike, Nucleocapsid and Membrane
397 proteins of SARS-CoV-2 (final peptide concentration 1 μ g/ml/peptide, Miltenyi Biotech) and
398 an unstimulated and positive control mix (containing anti-CD3 (Mabtech AB),
399 Staphylococcus Enterotoxin B (SEB), Phytohaemagglutinin (PHA) (all Sigma Aldrich)) at
400 37°C in a humidified CO₂ atmosphere for 48 hours. The cells and medium were decanted
401 from the plate and the assay developed following the manufacturer's instructions. Developed
402 plates were read using an AID iSpot reader (Oxford Biosystems, Oxford, UK) and counted
403 using AID EliSpot v7 software (Autoimmun Diagnostika GmbH, Strasberg, Germany). All
404 data were then corrected for background cytokine production and expressed as SFU/Million
405 PBMC or CD3 T cells.

406

407 *MAbs pseudovirus neutralization assay*

408 MLV-based SARS-CoV-2 S-glycoprotein-pseudotyped viruses were prepared as previously
409 described (Pinto et al., 2020). HEK293T/17cells were cotransfected with a WT or B.1.1.7
410 SARS-CoV-2 Spike glycoprotein-encoding-plasmid, an MLV Gag-Pol packaging construct
411 and the MLV transfer vector encoding a luciferase reporter using X-tremeGENE HP
412 transfection reagent (Roche) according to the manufacturer's instructions. Cells were cultured
413 for 72 h at 37°C with 5% CO₂ before harvesting the supernatant. VeroE6 stably expressing
414 human TMPRSS2 were cultured in DMEM containing 10% FBS, 1% penicillin-
415 streptomycin, 8 μ g/mL puromycin and plated into 96-well plates for 16–24 h. Pseudovirus
416 with serial dilution of mAbs was incubated for 1 h at 37°C and then added to the wells after
417 washing 2 times with DMEM. After 2–3 h DMEM containing 20% FBS and 2% penicillin-

418 streptomycin was added to the cells. Following 48-72 h of infection, Bio-Glo (Promega) was
419 added to the cells and incubated in the dark for 15 min before reading luminescence with
420 Synergy H1 microplate reader (BioTek). Measurements were done in duplicate and relative
421 luciferase units were converted to percent neutralization and plotted with a non-linear
422 regression model to determine IC₅₀ values using GraphPad PRISM software (version 9.0.0).

423

424 *Antibody binding measurements using bio-layer interferometry (BLI)*

425 MAbs were diluted to 3 µg/ml in kinetic buffer (PBS supplemented with 0.01% BSA) and
426 immobilized on Protein A Biosensors (FortéBio). Antibody-coated biosensors were
427 incubated for 3 min with a solution containing 5 µg/ml of WT or N50Y SARS-CoV-2
428 RBD in kinetic buffer, followed by a 3-min dissociation step. Change in molecules bound to
429 the biosensors caused a shift in the interference pattern that was recorded in real time using
430 an Octet RED96 system (FortéBio). The binding response over time was used to calculate
431 the area under the curve (AUC) using GraphPad PRISM software (version 9.0.0).

432

433 *Production of SARS-CoV-2 and B.1.1.7 receptor binding domains and human ACE2*

434 The SARS-CoV-2 RBD (BEI NR-52422) construct was synthesized by GenScript into
435 CMVR with an N-terminal mu-phosphatase signal peptide and a C-terminal octa-histidine tag
436 (GHHHHHHHH) and an avi tag. The boundaries of the construct are N₃₂₈RFPN₃₃₁ and
437 ₅₂₈KKST₅₃₁-C⁴⁹. The B.1.1.7 RBD was synthesized by GenScript into pCMVR with the same
438 boundaries and construct details with a mutation at N501Y. These plasmids were transiently
439 transfected into Expi293F cells using Expi293F expression medium (Life Technologies) at
440 37°C 8% CO₂ rotating at 150 rpm. The cultures were transfected using PEI cultivated for
441 5 days. Supernatants were clarified by centrifugation (10 min at 4000xg) prior to loading onto
442 a nickel-NTA column (GE). Purified protein was biotinylated overnight using BirA (Avidity)
443 prior to SEC into PBS. Human ACE2-Fc (residues 1-615 with a C-terminal thrombin
444 cleavage site and human Fc tag) were synthesized by Twist. Clarified supernatants were
445 affinity purified using a Protein A column (GE LifeSciences) directly neutralized and buffer
446 exchanged. The Fc tag was removed by thrombin cleavage in a reaction mixture containing
447 3 mg of recombinant ACE2-FC ectodomain and 10 µg of thrombin in 20 mM Tris-HCl
448 pH8.0, 150 mM NaCl and 2.5 mM CaCl₂. The reaction mixture was incubated at 25°C
449 overnight and re-loaded on a Protein A column to remove uncleaved protein and the Fc tag.
450 The cleaved protein was further purified by gel filtration using a Superdex 200 column
451 10/300 GL (GE Life Sciences) equilibrated in PBS.

452

453 *Protein affinity measurement using bio-layer interferometry*

454 Biotinylated RBD (either WT or N501Y) were immobilized at 5 ng/uL in undiluted 10X
455 Kinetics Buffer (Pall) to SA sensors until a load level of 1.1nm, A dilution series of either
456 monomeric ACE2 or Fab in undiluted kinetics buffer starting at 1000-50nM was used for
457 300-600 seconds to determine protein-protein affinity. The data were baseline subtracted and
458 the plots fitted using the Pall FortéBio/Sartorius analysis software (version 12.0). Data were
459 plotted in Prism.

460

461

462 **Supplementary Table 1: Vaccinee Participant ages**

ID	Age
1	60-65
2	80-85
3	40-45
4	85-90
5	25-30
6	35-40
7	80-85
8	80-85
9	55-60
10	85-90
11	80-85
12	80-85
13	80-85
14	85-90
15	75-80
16	80-85
17	80-85
18	85-90
19	85-90
20	80-85
22	55-60
25	60-65

463

464

465

466

467

468

469

470 **Table 2. Kinetic analysis of human ACE2 binding to SARS-CoV-2 B.1.1.7 and Wuhan-1**
471 **RBDs by bilayer interferometry.** Values reported represent the global fit to the data shown
472 in Extended Data Fig. 7.

		SARS-CoV-2 RBD WT	SARS-CoV-2 RBD B.1.1.7
K_D (nM)		133	22
k_{on} ($M^{-1}.s^{-1}$)	hACE2	$1.3 \cdot 10^5$	$1.4 \cdot 10^5$
k_{off} (s^{-1})		$1.8 \cdot 10^{-2}$	$3 \cdot 10^{-3}$

473

474

475

476

477

478

Extended Data Table 1. Neutralization, V gene usage and other properties of tested mAbs.

mAb	Domain (site)	VH usage (% id.)	Source (DSO)	IC50 WT (ng/ml)	IC50 B.1.1.7 (ng/ml)	ACE2 blocking	SARS-CoV	Escape residues	Ref.
4A8	NTD (i)	1-24	N/A	38	-	Neg.	-	S12P; C136Y; Y144del; H146Y; K147T; R246A	⁵⁰
S2L26	NTD (i)	1-24 (97.2)	Hosp. (52)	70	-	Neg.	-	N/A	²²
S2L50	NTD (i)	4-59 (95.4)	Hosp. (52)	264	50	Neg.	-	N/A	²²
S2M28	NTD (i)	3-33 (97.6)	Hosp. (46)	295	12'207	Neg.	-	P9S/Q; S12P; C15F/R; L18P; Y28C; A123T; C136Y; G142D; Y144del; K147Q/T; R246G; P251L; G252C	²²
S2X107	NTD (i)	4-38-2 (97)	Sympt. (75)	388	-	Neg.	-	N/A	²²
S2X124	NTD (i)	3-30 (99)	Sympt. (75)	221	-	Neg.	-	N/A	²²
S2X158	NTD (i)	1-24 (96.3)	Sympt. (75)	56	-	Neg.	-	N/A	²²
S2X28	NTD (i)	3-30 (97.9)	Sympt. (48)	1'399	-	Neg.	-	P9S; S12P; C15W; L18P; C136G/Y; F140S; L141S; G142C/D; Y144C/N; K147T/Q/E; R158G; L244S; R246G	²²
S2X303	NTD (i)	2-5 (95.9)	Sympt. (125)	69	-	Neg.	-	N/A	²²
S2X333	NTD (i)	3-33 (96.5)	Sympt. (125)	66	-	Neg.	-	P9L; S12P; C15S/Y; L18P; C136G/Y; F140C; G142D; K147T	²²
S2D106	RBD (I/RBM)	1-69 (97.2)	Hosp. (98)	27	20	Strong	-	N/A	⁸
S2D19	RBD (I/RBM)	4-31 (99.7)	Hosp. (49)	128	75'200	Moderate	-	N/A	⁸
S2D32	RBD (I/RBM)	3-49 (98.3)	Hosp. (49)	26	11	Strong	-	N/A	⁸
S2D65	RBD (I/RBM)	3-9 (96.9)	Hosp. (49)	24	12	Weak	-	N/A	⁸
S2D8	RBD (I/RBM)	3-23 (96.5)	Hosp. (49)	27	58'644	Strong	-	N/A	⁸
S2D97	RBD (I/RBM)	2-5 (96.9)	Hosp. (98)	20	17	Weak	-	N/A	⁸
S2E11	RBD (I/RBM)	4-61 (98.3)	Hosp. (51)	27	16	Weak	-	N/A	⁸
S2E12	RBD (I/RBM)	1-58 (97.6)	Hosp. (51)	27	31	Strong	-	G476S (3x)	^{8,51}
S2E13	RBD (I/RBM)	1-18 (96.2)	Hosp. (51)	34	77	Strong	-	N/A	⁸
S2E16	RBD (I/RBM)	3-30 (98.3)	Hosp. (51)	36	38	Strong	-	N/A	⁸
S2E23	RBD (I/RBM)	3-64 (96.9)	Hosp. (51)	139	180	Strong	-	N/A	⁸
S2H14	RBD (I/RBM)	3-15 (100)	Sympt. (17)	460	64'463	Weak	-	N/A	^{8,52}
S2H19	RBD (I/RBM)	3-15 (98.6)	Sympt. (45)	239	-	Weak	-	N/A	⁸
S2H58	RBD (I/RBM)	1-2 (97.9)	Sympt. (45)	27	14	Strong	-	N/A	⁸
S2H7	RBD (I/RBM)	3-66 (98.3)	Sympt. (17)	492	573	Weak	-	N/A	⁸
S2H70	RBD (I/RBM)	1-2 (99)	Sympt. (45)	147	65	Weak	-	N/A	⁸
S2H71	RBD (I/RBM)	2-5 (99)	Sympt. (45)	36	9	Moderate	-	N/A	⁸
S2M11	RBD (I/RBM)	1-2 (96.5)	Hosp. (46)	11	4	Weak	-	Y449N; L455F; E484K; E484Q; F490L; F490S; S494P	^{8,51}
S2N12	RBD	4-39 (97.6)	Hosp. (51)	76	40	Strong	-	N/A	⁸

	(I/RBM)								
S2N22	RBD (I/RBM)	3-23 (96.5)	Hosp. (51)	32	21	Strong	-	N/A	⁸
S2N28	RBD (I/RBM)	3-30 (97.2)	Hosp. (51)	72	21	Strong	-	N/A	⁸
S2X128	RBD (I/RBM)	1-69-2 (97.6)	Sympt. (75)	50	112	Strong	-	N/A	⁸
S2X16	RBD (I/RBM)	1-69 (97.6)	Sympt. (48)	45	103	Strong	-	N/A	⁸
S2X192	RBD (I/RBM)	1-69 (96.9)	Sympt. (75)	326	-	Weak	-	N/A	⁸
S2X227	RBD (I/RBM)	1-46 (97.9)	Sympt. (75)	26	14	Strong	-	N/A	
S2X246	RBD (I/RBM)	3-48 (96.2)	Sympt. (75)	35	30	Strong	-	N/A	
S2X30	RBD (I/RBM)	1-69 (97.9)	Sympt. (48)	32	53	Strong	-	N/A	⁸
S2X324	RBD (I/RBM)	2-5 (97.3)	Sympt. (125)	8	23	Strong	-	N/A	
S2X58	RBD (I/RBM)	1-46 (99)	Sympt. (48)	32	47	Strong	-	N/A	⁸
S2H90	RBD (II)	4-61 (96.6)	Sympt. (81)	77	32	Strong	+	N/A	⁸
S2H94	RBD (II)	3-23 (93.4)	Sympt. (81)	123	144	Strong	+	N/A	⁸
S2H97	RBD (V)	5-51 (98.3)	Sympt. (81)	513	248	Weak	+	N/A	
S2K15	RBD (II)	2-26 (99.3)	Sympt. (87)	361	235	0	+	N/A	
S2K21	RBD (II)	3-33 (96.2)	Sympt. (118)	201	189	0	+	N/A	
S2K30	RBD (II)	1-2 (97.2)	Sympt. (87)	185	134	0	+	N/A	
S2K63v2	RBD (II)	3-30-3 (95.6)	Sympt. (118)	144	215	0	+	N/A	
S2L17	RBD (?)	5-10-1 (98.3)	Hosp. (51)	313	127	Moderate	+	N/A	⁸
S2L37	RBD (II)	3-13 (98.3)	Hosp. (51)	14 ³ 70	824	Moderate	+	N/A	
S2L49	RBD (?)	3-30 (97.9)	Hosp. (51)	24	32	Neg.	+	N/A	⁸
S2X259	RBD (IIa)	1-69 (94.1)	Sympt. (75)	145	91	Moderate	+	N/A	
S2X305	RBD (?)	1-2 (95.1)	Sympt. (125)	34	21	Strong	-	N/A	
S2X35	RBD (IIa)	1-18 (98.6)	Sympt. (48)	140	143	Strong	+	N/A	⁵²
S2X450	RBD (?)	2-26 (96.9)	Sympt. (271)	368	198	Strong	+	N/A	
S2X475	RBD (?)	3-21 (93.8)	Sympt. (271)	1 ⁴ 31	851	Strong	+	N/A	
S2X607	RBD (?)	3-66 (95.4)	Sympt. (271)	41	23	Strong	-	N/A	
S2X608	RBD (?)	1-33 (93.2)	Sympt. (271)	21	35	Strong	-	N/A	
S2X609	RBD (?)	1-69 (93.8)	Sympt. (271)	47	35	Strong	-	N/A	
S2X613	RBD (?)	1-2 (91.7)	Sympt. (271)	28	19	Strong	-	N/A	
S2X615	RBD (?)	3-11 (94.8)	Sympt. (271)	23	17	Strong	-	N/A	
S2X619	RBD (?)	1-69 (92.7)	Sympt. (271)	36	60	Strong	-	N/A	
S2X620	RBD (?)	3-53 (95.1)	Sympt. (271)	34	45	Strong	-	N/A	

id., identity. DSO, days after symptom onset. * as described in Piccoli et al and McCallum et al. N/A, not available; -, not neutralizing

479

480

481

482 **References**

483

- 484 1 Zhou, P. *et al.* A pneumonia outbreak associated with a new coronavirus of probable
485 bat origin. *Nature* **579**, 270-273, doi:10.1038/s41586-020-2012-7 (2020).
- 486 2 Davies, N. G. *et al.* Estimated transmissibility and severity of novel SARS-CoV-2
487 Variant of Concern 202012/01 in England. *medRxiv*, 2020.2012.2024.20248822,
488 doi:10.1101/2020.12.24.20248822 (2020).
- 489 3 Volz, E. *et al.* Transmission of SARS-CoV-2 Lineage B.1.1.7 in England: Insights from
490 linking epidemiological and genetic data. *medRxiv*, 2020.2012.2030.20249034,
491 doi:10.1101/2020.12.30.20249034 (2021).
- 492 4 Korber, B. *et al.* Tracking Changes in SARS-CoV-2 Spike: Evidence that D614G
493 Increases Infectivity of the COVID-19 Virus. *Cell* **182**, 812-827 e819,
494 doi:10.1016/j.cell.2020.06.043 (2020).
- 495 5 Yurkovetskiy, L. *et al.* Structural and Functional Analysis of the D614G SARS-CoV-2
496 Spike Protein Variant. *Cell* **183**, 739-751 e738, doi:10.1016/j.cell.2020.09.032 (2020).
- 497 6 Martinot, M. *et al.* Remdesivir failure with SARS-CoV-2 RNA-dependent RNA-
498 polymerase mutation in a B-cell immunodeficient patient with protracted Covid-19.
499 *Clin Infect Dis*, doi:10.1093/cid/ciaa1474 (2020).
- 500 7 Kemp, S. *et al.* Neutralising antibodies in Spike mediated SARS-CoV-2 adaptation.
501 *medRxiv*, 2020.2012.2005.20241927, doi:10.1101/2020.12.05.20241927 (2020).
- 502 8 Thomson, E. C. *et al.* The circulating SARS-CoV-2 spike variant N439K maintains
503 fitness while evading antibody-mediated immunity. *bioRxiv*, 1-49,
504 doi:papers3://publication/doi/10.1101/2020.11.04.355842 (2020).
- 505 9 Baden, L. R. *et al.* Efficacy and Safety of the mRNA-1273 SARS-CoV-2 Vaccine. *N Engl*
506 *J Med*, doi:10.1056/NEJMoa2035389 (2020).
- 507 10 Polack, F. P. *et al.* Safety and Efficacy of the BNT162b2 mRNA Covid-19 Vaccine. *N*
508 *Engl J Med* **383**, 2603-2615, doi:10.1056/NEJMoa2034577 (2020).
- 509 11 Voysey, M. *et al.* Safety and efficacy of the ChAdOx1 nCoV-19 vaccine (AZD1222)
510 against SARS-CoV-2: an interim analysis of four randomised controlled trials in Brazil,
511 South Africa, and the UK. *Lancet* **397**, 99-111, doi:10.1016/S0140-6736(20)32661-1
512 (2021).
- 513 12 Mulligan, M. J. *et al.* Phase I/II study of COVID-19 RNA vaccine BNT162b1 in adults.
514 *Nature* **586**, 589-593, doi:10.1038/s41586-020-2639-4 (2020).
- 515 13 Corbett, K. S. *et al.* SARS-CoV-2 mRNA Vaccine Development Enabled by Prototype
516 Pathogen Preparedness. *bioRxiv*, 2020.2006.2011.145920,
517 doi:10.1101/2020.06.11.145920 (2020).
- 518 14 Folegatti, P. M. *et al.* Safety and immunogenicity of the ChAdOx1 nCoV-19 vaccine
519 against SARS-CoV-2: a preliminary report of a phase 1/2, single-blind, randomised
520 controlled trial. *Lancet* **396**, 467-478, doi:10.1016/S0140-6736(20)31604-4 (2020).
- 521 15 Kemp, S. A. *et al.* Recurrent emergence and transmission of a SARS-CoV-2 Spike
522 deletion ΔH69/V70. *bioRxiv*, 2020.2012.2014.422555,
523 doi:10.1101/2020.12.14.422555 (2020).
- 524 16 Tegally, H. *et al.* Emergence and rapid spread of a new severe acute respiratory
525 syndrome-related coronavirus 2 (SARS-CoV-2) lineage with multiple spike mutations
526 in South Africa. *medRxiv*, 2020.2012.2021.20248640,
527 doi:10.1101/2020.12.21.20248640 (2020).

- 528 17 Faria, N. R. *et al.* Genomic characterisation of an emergent SARS-CoV-2 lineage in
529 Manaus: preliminary findings, <[https://virological.org/t/genomic-characterisation-](https://virological.org/t/genomic-characterisation-of-an-emergent-sars-cov-2-lineage-in-manaus-preliminary-findings/586)
530 [of-an-emergent-sars-cov-2-lineage-in-manaus-preliminary-findings/586](https://virological.org/t/genomic-characterisation-of-an-emergent-sars-cov-2-lineage-in-manaus-preliminary-findings/586)> (2021).
- 531 18 Jackson, L. A. *et al.* An mRNA Vaccine against SARS-CoV-2 - Preliminary Report. *N*
532 *Engl J Med* **383**, 1920-1931, doi:10.1056/NEJMoa2022483 (2020).
- 533 19 Walsh, E. E. *et al.* Safety and Immunogenicity of Two RNA-Based Covid-19 Vaccine
534 Candidates. *New England Journal of Medicine* **383**, 2439-2450,
535 doi:10.1056/NEJMoa2027906 (2020).
- 536 20 Schmidt, F. *et al.* Measuring SARS-CoV-2 neutralizing antibody activity using
537 pseudotyped and chimeric viruses. 2020.2006.2008.140871,
538 doi:10.1101/2020.06.08.140871 %J bioRxiv (2020).
- 539 21 Brouwer, P. J. M. *et al.* Potent neutralizing antibodies from COVID-19 patients define
540 multiple targets of vulnerability. *Science* **369**, 643-650, doi:10.1126/science.abc5902
541 (2020).
- 542 22 McCallum, M. *et al.* N-terminal domain antigenic mapping reveals a site of
543 vulnerability for SARS-CoV-2. *bioRxiv*, doi:10.1101/2021.01.14.426475 (2021).
- 544 23 Walls, A. C. *et al.* Structure, Function, and Antigenicity of the SARS- CoV-2 Spike
545 Glycoprotein. *Cell* **181**, 281-292.e286,
546 doi:papers3://publication/doi/10.1016/j.cell.2020.02.058 (2020).
- 547 24 Guan, Y. *et al.* Isolation and characterization of viruses related to the SARS
548 coronavirus from animals in southern China. *Science* **302**, 276-278,
549 doi:10.1126/science.1087139 (2003).
- 550 25 Li, W. *et al.* Efficient replication of severe acute respiratory syndrome coronavirus in
551 mouse cells is limited by murine angiotensin-converting enzyme 2. *J Virol* **78**, 11429-
552 11433, doi:10.1128/JVI.78.20.11429-11433.2004 (2004).
- 553 26 Li, W. *et al.* Receptor and viral determinants of SARS-coronavirus adaptation to
554 human ACE2. *EMBO J* **24**, 1634-1643, doi:10.1038/sj.emboj.7600640 (2005).
- 555 27 Starr, T. N. *et al.* Deep Mutational Scanning of SARS-CoV-2 Receptor Binding Domain
556 Reveals Constraints on Folding and ACE2 Binding. *Cell* **182**, 1295-1310 e1220,
557 doi:10.1016/j.cell.2020.08.012 (2020).
- 558 28 Verschoor, C. P. *et al.* Microneutralization assay titres correlate with protection
559 against seasonal influenza H1N1 and H3N2 in children. *PloS one* **10**, e0131531,
560 doi:10.1371/journal.pone.0131531 (2015).
- 561 29 Kulkarni, P. S., Hurwitz, J. L., Simoes, E. A. F. & Piedra, P. A. Establishing Correlates of
562 Protection for Vaccine Development: Considerations for the Respiratory Syncytial
563 Virus Vaccine Field. *Viral Immunol* **31**, 195-203, doi:10.1089/vim.2017.0147 (2018).
- 564 30 Goddard, N. L., Cooke, M. C., Gupta, R. K. & Nguyen-Van-Tam, J. S. Timing of
565 monoclonal antibody for seasonal RSV prophylaxis in the United Kingdom. *Epidemiol*
566 *Infect* **135**, 159-162, doi:10.1017/S0950268806006601 (2007).
- 567 31 Mercado, N. B. *et al.* Single-shot Ad26 vaccine protects against SARS-CoV-2 in rhesus
568 macaques. *Nature* **586**, 583-588, doi:10.1038/s41586-020-2607-z (2020).
- 569 32 McMahan, K. *et al.* Correlates of protection against SARS-CoV-2 in rhesus macaques.
570 *Nature*, doi:10.1038/s41586-020-03041-6 (2020).
- 571 33 Wang, Z. *et al.* mRNA vaccine-elicited antibodies to SARS-CoV-2 and circulating
572 variants. *bioRxiv*, doi:10.1101/2021.01.15.426911 (2021).

- 573 34 Wu, K. *et al.* mRNA-1273 vaccine induces neutralizing antibodies against spike
574 mutants from global SARS-CoV-2 variants. *bioRxiv*, doi:10.1101/2021.01.25.427948
575 (2021).
- 576 35 Soh, W. T. *et al.* The N-terminal domain of spike glycoprotein mediates SARS-CoV-2
577 infection by associating with L-SIGN and DC-SIGN. 1-30,
578 doi:papers3://publication/doi/10.1101/2020.11.05.369264 (2020).
- 579 36 Wibmer, C. K. *et al.* SARS-CoV-2 501Y.V2 escapes neutralization by South African
580 COVID-19 donor plasma. *bioRxiv*, doi:10.1101/2021.01.18.427166 (2021).
- 581 37 Greaney, A. J. *et al.* Comprehensive mapping of mutations to the SARS-CoV-2
582 receptor-binding domain that affect recognition by polyclonal human serum
583 antibodies. *bioRxiv*, 2020.2012.2031.425021, doi:10.1101/2020.12.31.425021
584 (2021).
- 585 38 Greaney, A. J. *et al.* Complete mapping of mutations to the SARS-CoV-2 spike
586 receptor-binding domain that escape antibody recognition. *Cell Host & Microbe*
587 (2020).
- 588 39 Weisblum, Y. *et al.* Escape from neutralizing antibodies by SARS-CoV-2 spike protein
589 variants. *Elife* **9**, e61312, doi:10.7554/eLife.61312 (2020).
- 590 40 Corti, D. *et al.* A neutralizing antibody selected from plasma cells that binds to group
591 1 and group 2 influenza A hemagglutinins. *Science* **333**, 850-856,
592 doi:10.1126/science.1205669 (2011).
- 593 41 Pinto, D. *et al.* Cross-neutralization of SARS-CoV-2 by a human monoclonal SARS-CoV
594 antibody. *Nature* **583**, 290-295, doi:10.1038/s41586-020-2349-y (2020).
- 595 42 Tortorici, M. A. *et al.* Ultrapotent human antibodies protect against SARS-CoV-2
596 challenge via multiple mechanisms. *Science*, doi:10.1126/science.abe3354 (2020).
- 597 43 Gregson, J. *et al.* HIV-1 viral load is elevated in individuals with reverse transcriptase
598 mutation M184V/I during virological failure of first line antiretroviral therapy and is
599 associated with compensatory mutation L74I. *Journal of Infectious Diseases* (2019).
- 600 44 Forloni, M., Liu, A. Y. & Wajapeyee, N. Creating Insertions or Deletions Using Overlap
601 Extension Polymerase Chain Reaction (PCR) Mutagenesis. *Cold Spring Harb Protoc*
602 **2018**, doi:10.1101/pdb.prot097758 (2018).
- 603 45 Case, J. B. *et al.* Neutralizing Antibody and Soluble ACE2 Inhibition of a Replication-
604 Competent VSV-SARS-CoV-2 and a Clinical Isolate of SARS-CoV-2. *Cell Host Microbe*
605 **28**, 475-485 e475, doi:10.1016/j.chom.2020.06.021 (2020).
- 606 46 Naldini, L., Blomer, U., Gage, F. H., Trono, D. & Verma, I. M. Efficient transfer,
607 integration, and sustained long-term expression of the transgene in adult rat brains
608 injected with a lentiviral vector. *Proc Natl Acad Sci U S A* **93**, 11382-11388,
609 doi:10.1073/pnas.93.21.11382 (1996).
- 610 47 Gupta, R. K. *et al.* Full length HIV-1 gag determines protease inhibitor susceptibility
611 within in vitro assays. *AIDS* **24**, 1651 (2010).
- 612 48 Mlcochova, P. *et al.* Combined point of care nucleic acid and antibody testing for
613 SARS-CoV-2 following emergence of D614G Spike Variant. *Cell Rep Med*, 100099,
614 doi:10.1016/j.xcrm.2020.100099 (2020).
- 615 49 Walls, A. C. *et al.* Elicitation of Potent Neutralizing Antibody Responses by Designed
616 Protein Nanoparticle Vaccines for SARS-CoV-2. *Cell* **183**, 1367-1382 e1317,
617 doi:10.1016/j.cell.2020.10.043 (2020).

618 50 Chi, X. *et al.* A neutralizing human antibody binds to the N-terminal domain of the
619 Spike protein of SARS-CoV-2. *Science*, eabc6952-6913,
620 doi:papers3://publication/doi/10.1126/science.abc6952 (2020).
621 51 Tortorici, M. A. *et al.* Ultrapotent human antibodies protect against SARS-CoV-2
622 challenge via multiple mechanisms. *Science* **4**, eabe3354-3316,
623 doi:papers3://publication/doi/10.1126/science.abe3354 (2020).
624 52 Piccoli, L. *et al.* Mapping neutralizing and immunodominant sites on the SARS-CoV-2
625 spike receptor-binding domain by structure-guided high-resolution serology. *Cell*, 1-
626 55, doi:papers3://publication/doi/10.1016/j.cell.2020.09.037 (2020).
627

Figure 1

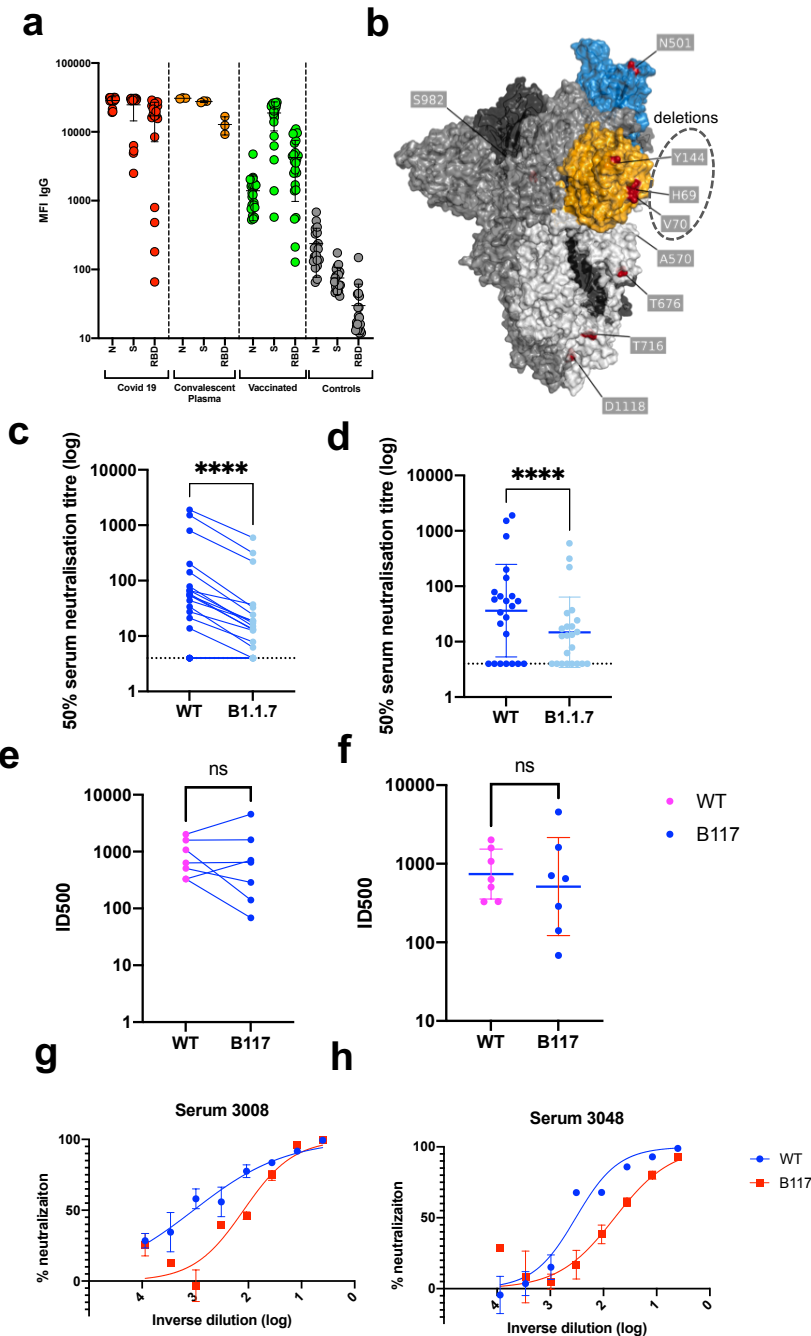


Figure 1. Neutralisation by sera against wild type and B.1.1.7 Spike mutant SARS-CoV-2 pseudotyped viruses. **a**, Serum IgG responses against N protein, Spike and the Spike Receptor Binding Domain (RBD) from 23 vaccinated participants (green), 20 recovered COVID-19 cases (red), 3 convalescent plasma units and 20 healthy controls (grey) as measured by a flow cytometry based Luminex assay. MFI, mean fluorescence intensity. **b**, Spike in open conformation with a single erect RBD (PDB: 6ZGG) in trimer axis vertical view with the locations of mutated residues highlighted in red spheres and labelled on the monomer with erect RBD. Vaccine (**c-d**) and convalescent sera (**e-f**) against WT and B.1.1.7 Spike mutant with N501Y, A570D, Δ H69/V70, Δ 144/145, P681H, T716I, S982A and D1118H. **g-h**, neutralisation curves for serum from two convalescent individuals with reduced susceptibility to B.1.1.7 Spike mutant, means of technical replicates are plotted with error bars representing standard error of mean. Data are representative of 2 independent experiments.

Figure 2

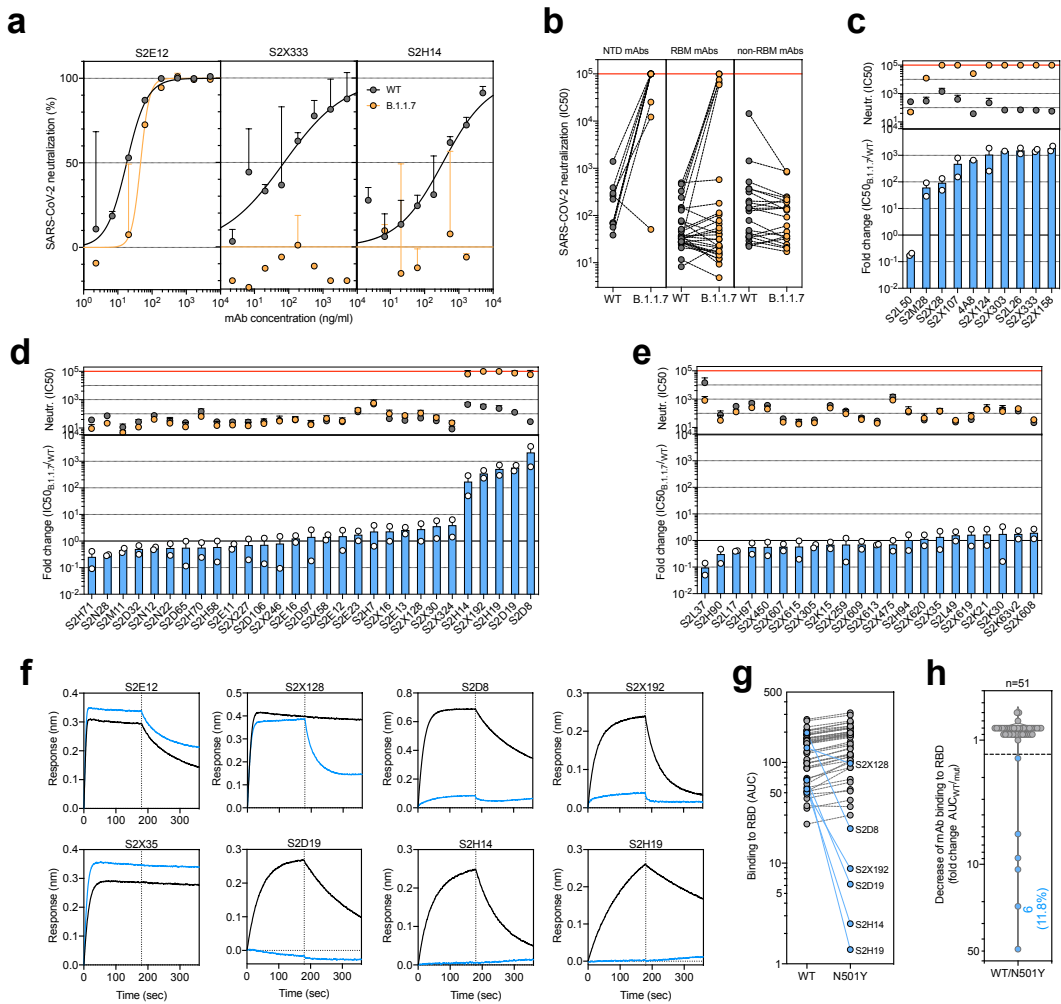


Figure 2. Neutralisation and binding by a panel of NTD- and RBD-specific mAbs against WT and B.1.1.7 SARS-CoV-2 viruses. **a**, Neutralisation of WT (black) and B.1.1.7 (orange) Spike pseudotyped SARS-CoV-2-MLV by 3 selected mAbs (S2E12, S2X333 and S2H14) from one representative experiment. Shown is the mean \pm s.d. of 2 technical replicates. **b**, Neutralisation of WT and B.1.1.7 SARS-CoV-2-MLV by 61 mAbs targeting NTD (n=10), RBM (n=29) and non-RBM sites in the RBD (n=22). Shown are the mean IC₅₀ values (ng/ml) of n=2 independent experiments. **c-e**, Neutralisation shown as mean IC₅₀ values (upper panel) and mean fold change of B.1.1.7 relative to WT (lower panel) of NTD (c), RBM (d) and non-RBM (e) mAbs. Lower panel shows IC₅₀ values from 2 independent experiments. **f-h**, Kinetics of binding of mAbs to WT (black) and N501Y (blue) RBD as measured by bio-layer interferometry (BLI). Shown in (f) are the 6 RBM-targeting mAbs with reduced binding to N501Y RBD and 2 representative mAbs (RBM-targeting S2E12 and non-RBM-targeting S2X35). Area under the curve (AUC) (g) and AUC fold change (h) of 51 mAbs tested against WT and N501Y RBD. mAbs with a >1.3 AUC fold change shown in blue.

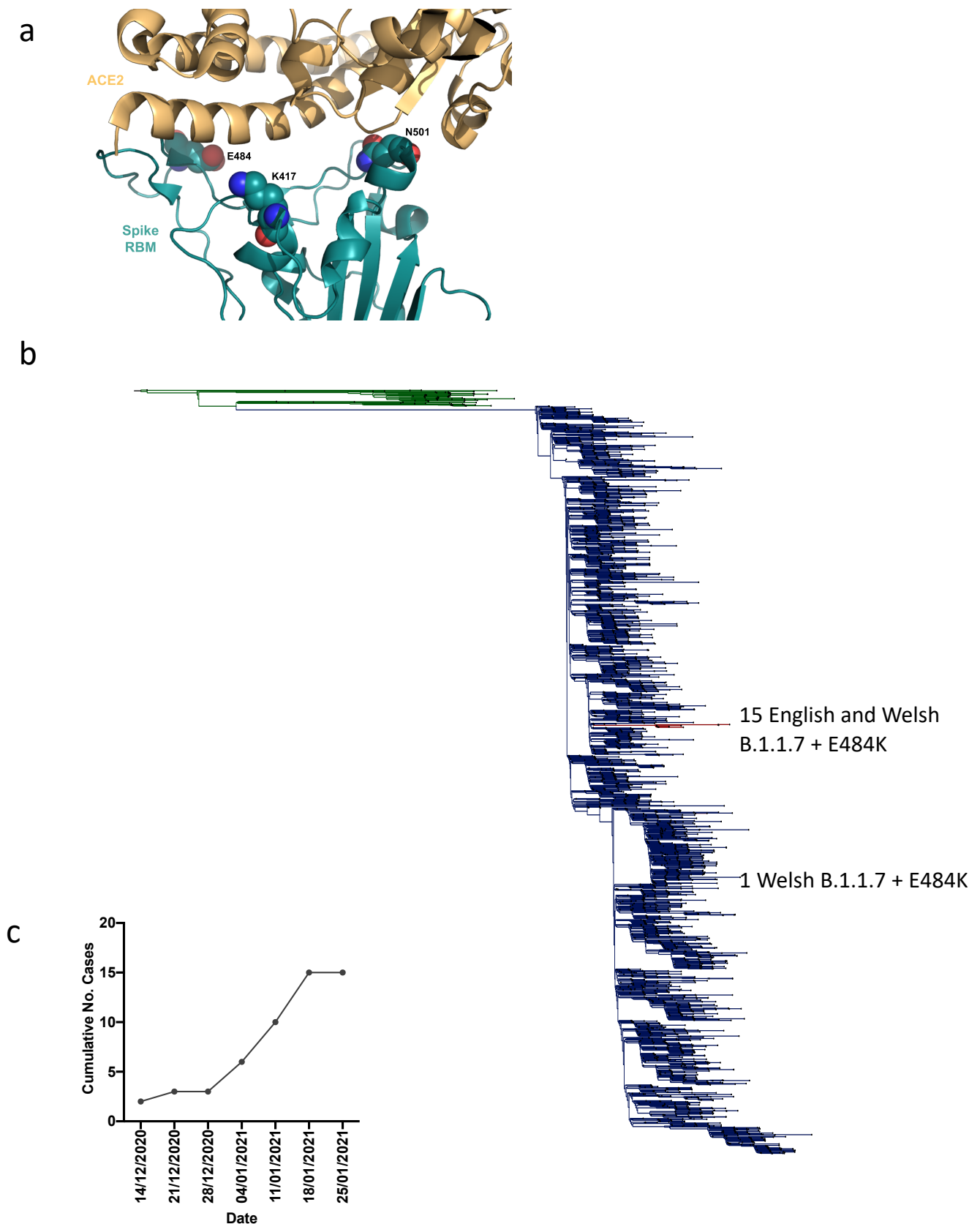
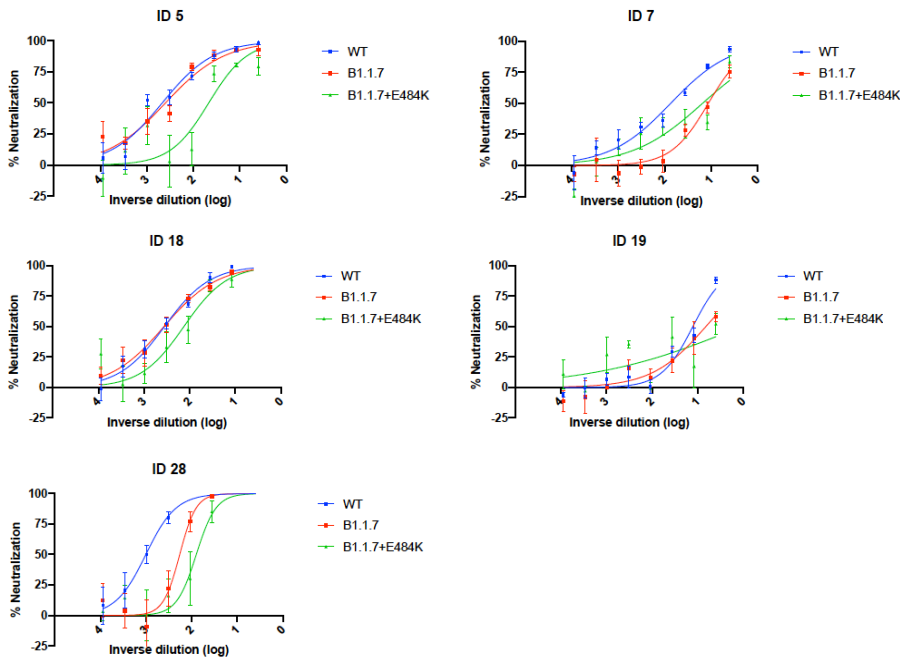


Figure 3. E484K appearing in background of B.1.1.7 with evidence of transmission a.

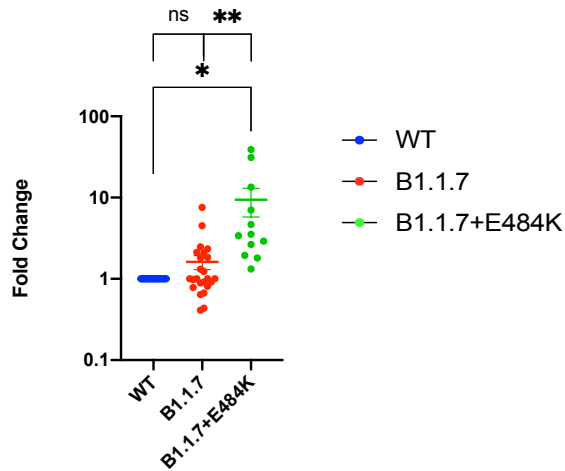
Representation of Spike RBM:ACE2 interface (PDB: 6M0J) with residues E484, N501 and K417 highlighted as spheres coloured by element **b**. Maximum likelihood phylogeny of a subset of sequences from the United Kingdom bearing the E484K mutation (green) and lineage B.1.1.7 (blue). As of 1st Feb 2021, 16 sequences from the B.1.1.7 lineage (two unrelated sequences in Wales, and one cluster of 14 in England) have acquired the E484K mutation (red). **c**. Sequence accumulation over time in GISAID for sequences with B.1.1.7 and E484K.

Figure 4

a



b



c

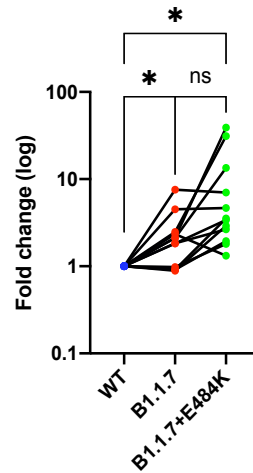
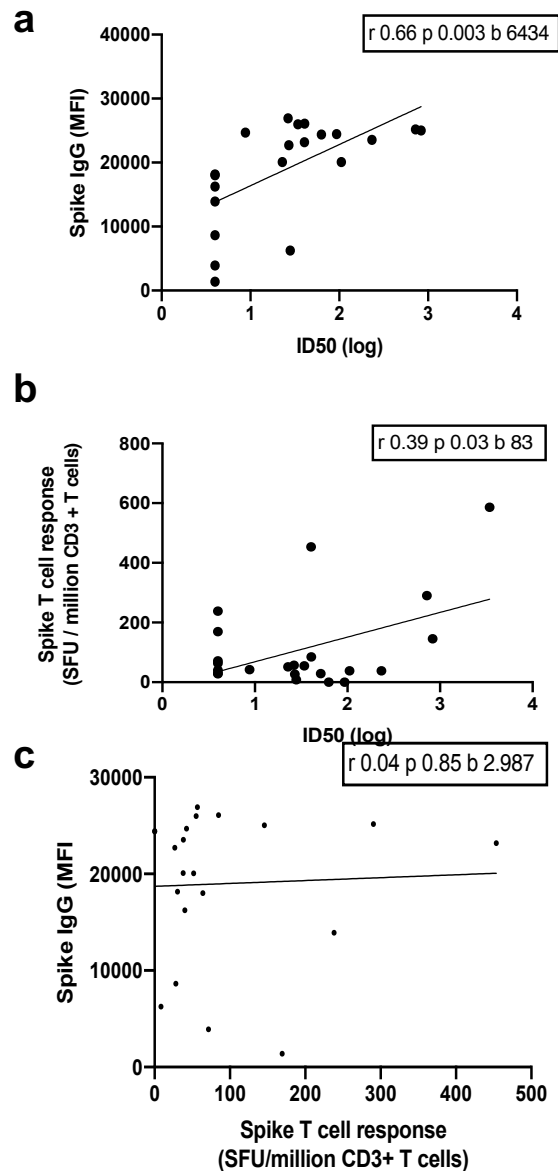


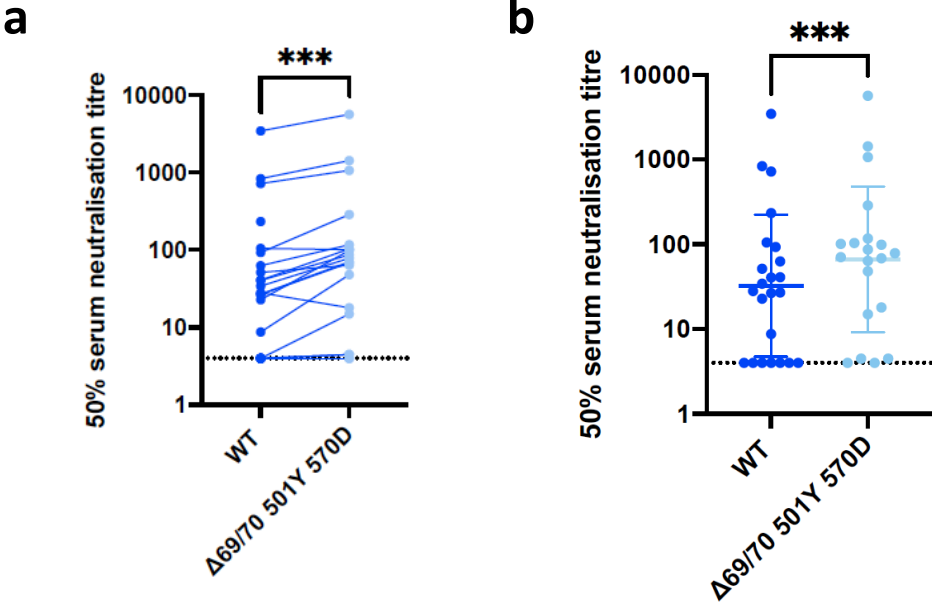
Figure 4. Neutralisation potency of vaccine sera against pseudovirus bearing Spike mutations in the B1.1.7 lineage with and without E484K in the receptor binding domain (all In Spike D614G background). **a**, Neutralisation curves for five vaccinated individuals. Data points represent mean of technical replicates with standard error and are representative of two independent experiments **b**, **c**. Indicated is 50% neutralisation titre for each virus expressed as fold change relative to WT. WT (n=24), B.1.1.7 (n=24), B.1.1.7 +E484K (n=12). In **c** only data for participants with FC from three viruses are presented. Data points represent means of two independent experiments.

Extended Data Figure 1



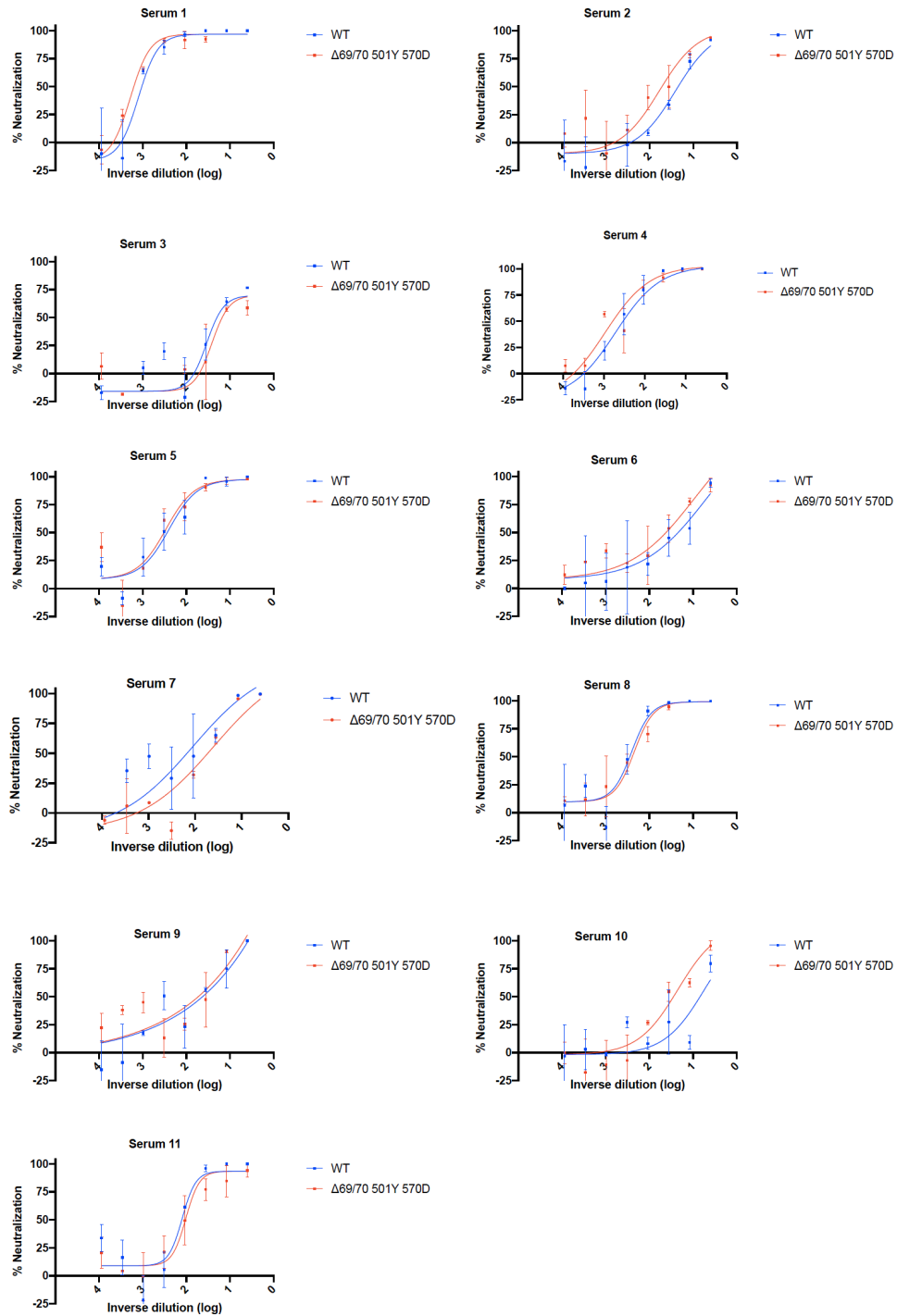
Extended Data Figure 1: Immune responses three weeks after first dose of Pfizer SARS-CoV-2 vaccine BNT162b2 **a**, Relationship between serum IgG responses as measured by flow cytometry and serum neutralisation ID50. **b**, Relationship between serum neutralisation ID50 and T cell responses against SARS-CoV-2 by IFN gamma ELISPOT. SFU: spot forming units. **c**, Relationship between serum IgG responses and T cell responses.

Extended Data Fig. 2



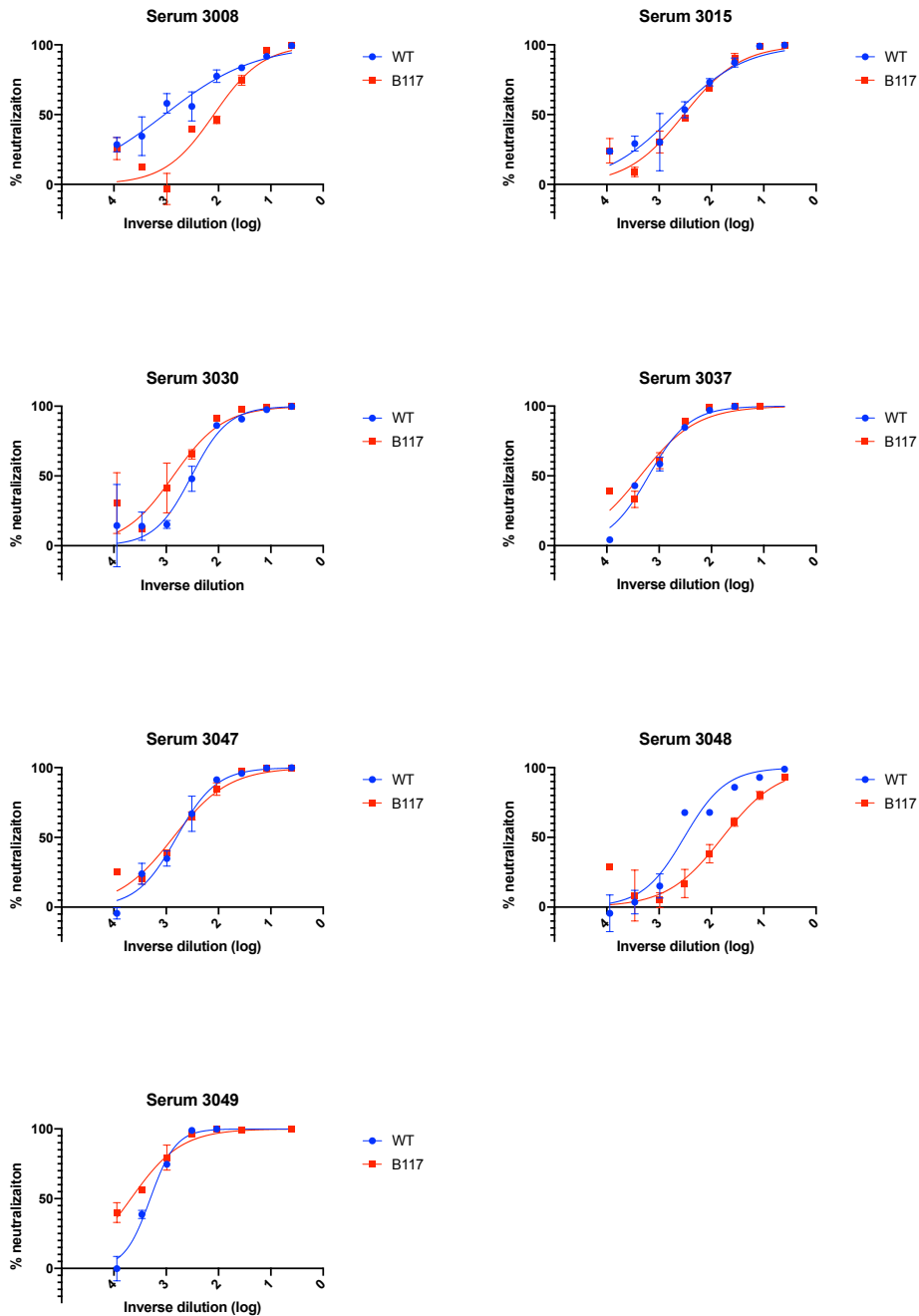
Extended data Fig 2. Neutralisation by vaccine sera against wild type and mutant SARS-CoV-2 pseudotyped viruses: (a-b) WT and Spike mutant with N501Y, A570D, Δ H69/V70. Data are representative of 2 independent experiments.

Extended Data Fig. 3



Extended Data Fig. 3. Neutralisation potency of convalescent sera against pseudovirus bearing three Spike mutations (N501Y, A570D, Δ H69/V70) present in B.1.1.7 versus wild type (all In Spike D614G background). Indicated is serum log₁₀ inverse dilution against % neutralisation. Where a curve is shifted to the right this indicates the virus is less sensitive to the neutralising antibodies in the serum. Data points represent means of technical replicates and error bars represent standard error of the mean.

Extended Data Fig. 4



Extended Data Fig. 4. Neutralisation potency of convalescent sera against wild type and B.1.1.7 Spike mutant SARS-CoV-2 pseudoviruses. Indicated is serum log₁₀ inverse dilution against % neutralisation. Where a curve is shifted to the right this indicates the virus is less sensitive to the neutralising antibodies in the serum. Data points represent means of technical replicates and error bars represent standard error of the mean.

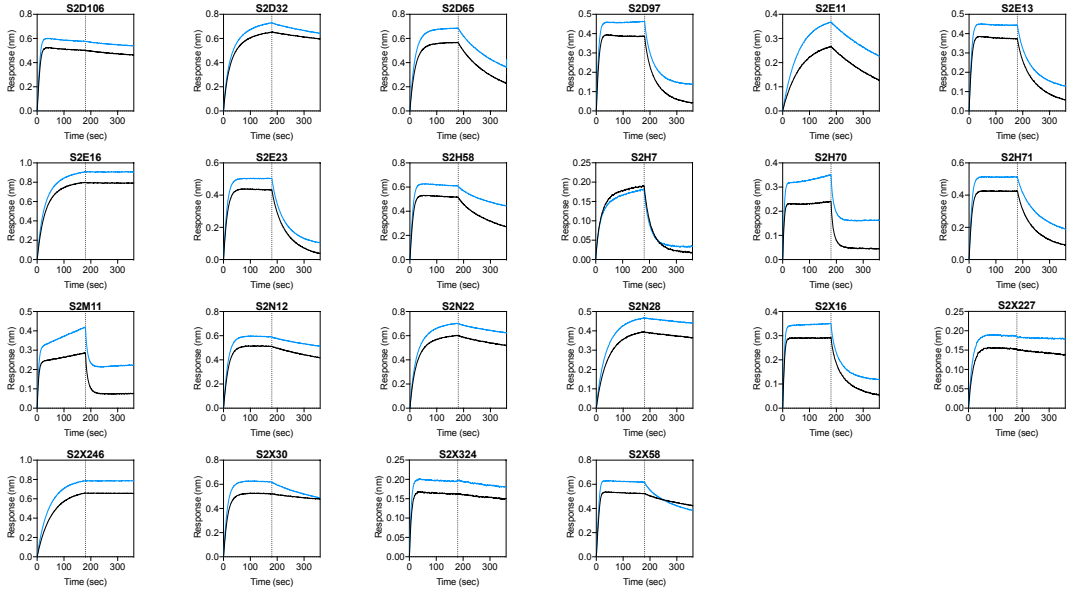
Extended Data Fig. 5



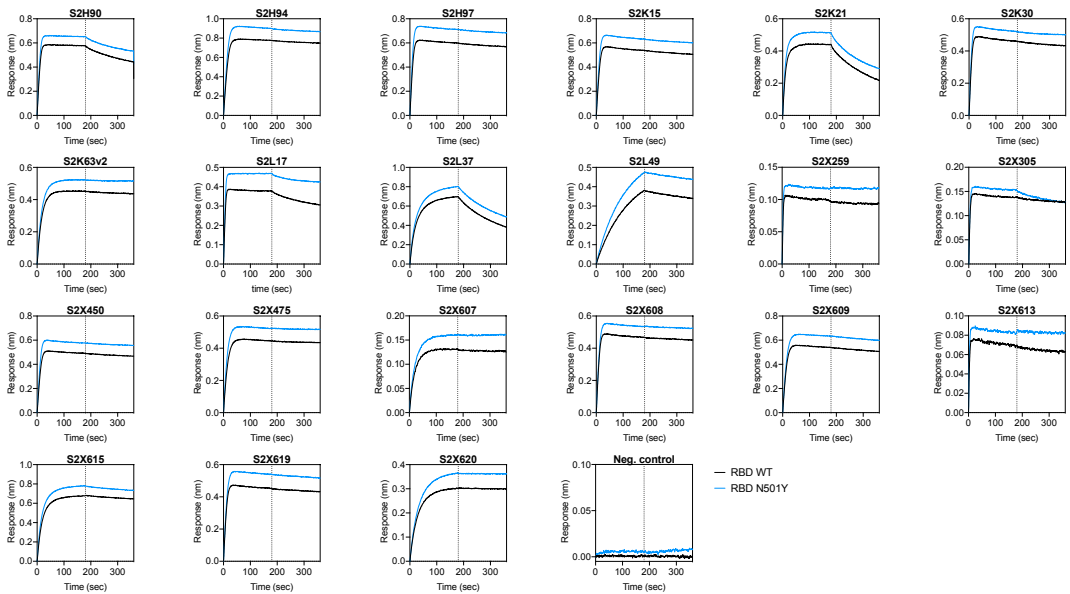
Extended Data Fig. 5. Neutralisation of WT and B.1.1.7 SARS-CoV-2 of a panel of 58 mAbs. **a-c**, Neutralisation of WT (black) and B.1.1.7 (orange) SARS-CoV-2-MLV by 9 NTD-targeting (a), 27 RBM-targeting (b) and 22 non-RBM-targeting (c) mAbs.

Extended Data Fig. 6

a

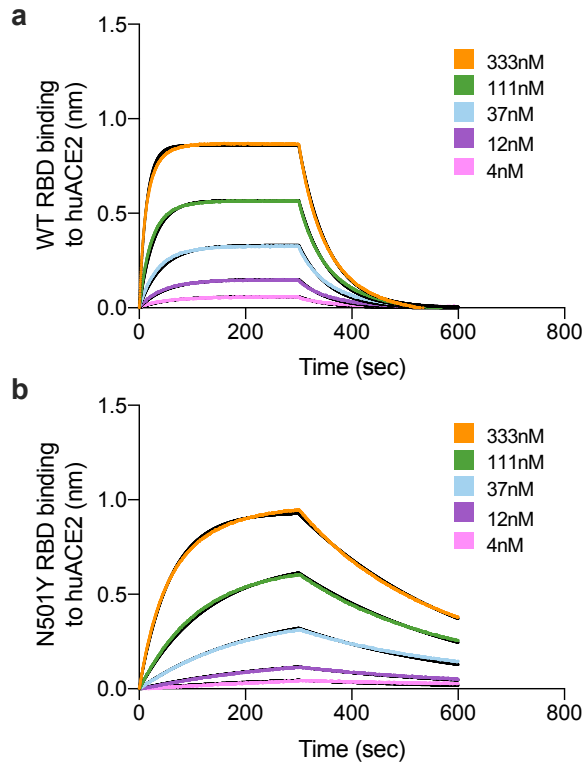


b



Extended Data Fig. 6. Kinetics of binding to WT and N501Y SARS-CoV-2 RBD of 43 RBD-specific mAbs. a-b, Binding to WT (black) and N501Y (blue) RBD by 22 RBM-targeting (a) and 21 non-RBM-targeting (b) mAbs. An antibody of irrelevant specificity was included as negative control.

Extended Data Fig. 7



Extended Data Fig. 7. Binding of human ACE2 to SARS-CoV-2 B.1.1.7 and WT RBDs. a-b. BLI binding analysis of the human ACE2 ectodomain (residues 1-615) to immobilized SARS-CoV-2 WT RBD (a) and B.1.1.7 RBD (b). Black lines correspond to a global fit of the data using a 1:1 binding model.